Generalized quantum Fokker–Planck theory and its application to laser driven intramolecular hydrogen transfer reactions in condensed phases

Oliver Kühn[a] and Yi Zhao[b]
Institut für Chemie, Physikalische und Theoretische Chemie, Freie Universität Berlin, Takustrasse 3, D-14195 Berlin, Germany

Feng Shuang and YiJing Yan
Department of Chemistry, Hong Kong University of Science and Technology, Kowloon, Hong Kong, China and Open Laboratory of Bond-Selective Chemistry, University of Science and Technology of China, Hefei, China

(Received 28 October 1999; accepted 20 January 2000)

A generalized quantum Fokker–Planck theory is proposed to treat the correlated dynamics of coherent driving and Markovian dissipation. The resulting formulation is applicable to arbitrary external time-dependent driving fields and satisfies the detailed balance condition at arbitrary temperatures. Analyzed are also the formal relations among the Caldeira–Leggett quantum Fokker–Planck equation, the Bloch–Redfield theory, and the present formulation. The approach is numerically implemented to study the intramolecular hydrogen transfer reaction dynamics in a one-dimensional model system. Different forms of external pulsed driving fields are exploited and their ability to compete with concurring relaxation processes is investigated. Energy relaxation and pure dephasing are shown to have rather different influences on the reaction yield. © *2000 American Institute of Physics.* [S0021-9606(00)51114-3]

I. INTRODUCTION

Quantum dissipation in the presence of a time-dependent strong excitation field remains a challenge in theoretical statistical dynamics (for a recent review, see Ref. 1). The combined effect of dissipation and external driving is most naturally incorporated in the path integral formalism. Here, in particular the development of iterative propagation schemes has opened the possibility to investigate the regime of non-Markovian dynamics.[2] The monochromatic driving of dissipative two-level systems[3–5] has been studied in detail, putting emphasis on the large amplitude transport or stabilization of localized states by the driving field. The cooperativity between driving and dissipation has been demonstrated in the context of stochastic resonance in which the response of a system to the periodic driving field exhibits maxima at certain strengths of dissipation.[6–8] The real-time path integral approach was also applied to the driving of a model hydrogen transfer reaction by means of ultrashort laser pulses.[9] The step towards laser driving of real multilevel systems requires, however, to abandon the exact treatment of the system–bath interaction provided by the path integral formulation. In the case of a few weakly coupled zeroth-order system states, e.g., in a curve crossing model, it has been shown that a canonical transformation can be used to separate the Franck–Condon weighted tunnel coupling matrix elements as small parameters.[10] Analysis of the transfer rates between the zeroth-order states then revealed the possibility of population control by means of external monochromatic fields.

There are also a number of investigations based on the Liouville equation or the generalized master equation (GME) for reduced density operators. In the context of laser control, both Markovian[11] and non-Markovian[12] dissipative media or baths have been used. The GME may be symbolically expressed as ($\hbar=1$)

$$\dot{\rho}=-i[H,\rho]-\mathcal{R}\rho. \tag{1}$$

Here, the first term describes the coherent dynamics governed by the Hamiltonian H of the reduced (relevant) system and its interaction with the driving field. The second term contains the superoperator $\mathcal{R}$ (dissipation tensor). However, it depends not only on the dissipation parameters but also on the Hamiltonian of the driven relevant system. This leads to a correlated dynamics of driving and dissipation. The formal expression for $\mathcal{R}$ can be derived by using the standard Zwanzig–Mori projection operator technique.[13–17] Usually, the interaction between the driven relevant system and its dissipative environment is treated using second-order perturbation theory.[17] In principle, the time-dependence of the dissipation tensor $\mathcal{R}$ arises from both, the non-Markovian behavior of the bath correlation function and the time-dependent external driving field.

The question arises how the interplay between driving and dissipation on a quantum system can be formulated in a manner that is not only theoretically correct but also numerically implementable. This point was addressed for a harmonic oscillator system by Graham *et al.*[18] They found in particular generalized quasi-energy states for which the

[a]Electronic mail: ok@chemie.fu-berlin.de
[b]Author to whom correspondence should be addressed; electronic mail: yi@chemie.fu-berlin.de

steady state solution to the density matrix is diagonal. These states interpolate between the Floquet states available for periodically driven conservative systems[1] and field-free system states. The issue of simultaneous driving and damping described by a GME in the Markovian limit was also discussed in Ref. 19. The density matrix theory formulated in the Floquet representation was applied to the dissipative tunneling in a double minimum potential in Ref. 20. A formulation based on the field-free system states has also been constructed.[8,21] Here, the combined influence of driving and dissipation is incorporated in time-dependent but Markovian dissipation operators. Applications are made to the transport in a periodically driven two-level system in Ref. 8, and to the optical transition in a displaced two-surface harmonic system in Ref. 21.

The above mentioned methods are all based on a specific state representation of the GME [Eq. (1)] which, in the field-free case, is known as the Redfield approach.[22–24] An alternative approach to the GME is the so-called generalized quantum Fokker–Planck (GQFP) theory. A Markovian Fokker–Planck theory was first developed by Dekker,[25–27] and later rederived and modified by Caldeira and Leggett.[28] While the Markovian limit results in an equation of motion for the reduced density operator ρ, the case of non-Markovian dissipation, covered by the GQFP approach, gives coupled equations of motion for ρ and a hierarchical set of auxiliary operators. The hierarchical GQFP approach was first taken by Tanimura and co-workers[29–32] for a Gaussian–Markovian bath. An application has been made to the transient absorption spectroscopy of a model three-surface system with a strong pump excitation.[33] Recently, Yan constructed a different type of hierarchical GQFP equations for the reduced dynamics in a model non-Gaussian–Markovian bath.[34] In the GQFP equation approach the Hamiltonian of the reduced system in the presence of the driving field governs the coherent dynamics of both the reduced density operator and the set of auxiliary dissipation operators. Thus it provides a theoretical foundation to study driven dissipative dynamics. However, the previous GQFP theory involves a high-temperature approximation based on a certain type of semiclassical fluctuation–dissipation relation.[28–34]

In this work we propose a modified Markovian GQFP theory which is applicable for arbitrary temperatures at least in the long time region. For very short times, the Markov approximation may break down itself. The formalism is applied to describe the correlated dynamics of external driving and dissipation. A numerical implementation is made to investigate laser driven intramolecular hydrogen transfer events (an isomerization reaction) in a one-dimensional model system with Markovian dissipation.

The remainder of this paper is organized as follows. Section II presents an overview of GME in a generalized Langevin description of system–bath coupling. We further use the Langevin GME to identify the energy relaxation rates $(1/T_1)$ and the coherence dephasing rates $(1/T_2)$ via dissipative system modes without invoking any specific representation. The Langevin GME also constitutes the basis for the main theoretical result of this paper, i.e., a modified Markovian GQFP formulation, to be developed in Sec. III. The resulting formulation is analyzed and compared with the Caldeira–Leggett equation[23] and the generalized Redfield theory[24,35] which will also be introduced in due course. In Sec. IV the modified Markovian GQFP equation is recast in the energy eigenstate representation. The Redfield tensor elements for both T_1-type relaxation and T_2-type dephasing dynamics are then examined explicitly. The results of the numerical implementation of the GQFP equation to the study of laser driven intramolecular hydrogen transfer reactions in a model system is made in Sec. V. Elucidated are the different effects of T_1-type relaxation and T_2-type dephasing on the yield of the laser-driven reaction. Finally, Sec. VI summarizes the paper.

II. GENERALIZED MASTER EQUATION AND LANGEVIN DISSIPATION MODES

In this section, we shall present some theoretical background of the GME in the presence of a time-dependent external field using a generalized Langevin description for the system–bath interaction. The resulting Langevin GME will be shown to have the following properties. First, it computationally reduces the tensor algebra of $\mathcal{R}$ in Eq. (1) to matrix multiplications (cf. Sec. II A). Second, it allows to identify various dissipation processes, especially the pure dephasing dynamics, in terms of system operators (cf. Sec. II B). Finally, it constitutes the foundation for the development of the generalized quantum Fokker–Planck equations[34] (cf. Sec. III).

A. Langevin generalized master equation

Consider a molecule embedded in a heat bath and driven by an external laser via the semiclassical dipole-field interaction, $-\mu\mathcal{E}(t)$ (μ is the dipole operator for the relevant system). The external field does not interact directly with the bath. The total Hamiltonian in a stochastic description assumes the form

$$H_{\mathrm{T}}(t)=H(t)+H_{\mathrm{SB}}(t), \tag{2}$$

with

$$H(t)=H_0-\mu\mathcal{E}(t), \tag{3a}$$

$$H_{\mathrm{SB}}(t)=-\sum_{\alpha} Q_{\alpha}F_{\alpha}(t). \tag{3b}$$

Here, $H(t)$ is the deterministic Hamiltonian which governs the coherent dynamics of the reduced molecular system in the presence of the external field $\mathcal{E}(t)$. $H_{\mathrm{SB}}(t)$ denotes the system–bath (SB) interaction and is of stochastic nature. Specifically the stochastic system–bath interaction is decomposed into a sum where each term contains a generalized system coordinate Q_{α} and the respective Langevin force $F_{\alpha}(t)$. We shall later relate the generalized system coordinate Q_{α}, which may also be termed as the *dissipative mode*, to the nature of its associated dissipation process (cf. Sec. II B). The generalized Langevin force $F_{\alpha}(t)$ is assumed to be a stationary Gaussian stochastic Hermitian operator in the bath space. Without loss of generality, we can set $\langle F_{\alpha}(t)\rangle=0$. Here, $\langle\cdots\rangle$ denotes the average over the initial

bath ensemble. The dynamic effect of bath is then completely determined by the two-time correlation function of the stochastic force[36]

$$\langle F_\alpha(t+\tau)F_{\alpha'}(\tau)\rangle = C_\alpha(t)\,\delta_{\alpha\alpha'}. \tag{4}$$

In this equation and hereafter, we assume that the Langevin forces on different dissipative modes are statistically independent. The correlation function obeys the relation $C_\alpha(-t)=C_\alpha^*(t)$. Furthermore, the detailed-balance or fluctuation–dissipation theorem requires that $C_\alpha^*(t)=C_\alpha(t-i\beta)$ or equivalently $\hat{C}_\alpha(-\omega)=e^{-\beta\omega}\hat{C}_\alpha(\omega)$ for its spectrum ($\beta\equiv\hbar/(k_BT)$).[37]

In the following theoretical development we adopt the initial factorization approximation, $\rho_T(0)=\rho(0)\rho_B(0)$, and assume that the system–bath interaction $H_{SB}(t)$ is weak compared with $H(t)$. As it was pointed out in Ref. 34, different resummation schemes for approximating the effect of higher orders in H_{SB} might result in different GMEs. In a simple second-order cumulant expansion formulation, the resulting GME is characterized by a time-local relaxation kernel without memory. With the Langevin description [Eq. (3b)], the final time-local GME reads as[34]

$$\dot{\rho} = -i[H(t),\rho] - \sum_\alpha [Q_\alpha, K_\alpha(t)\rho - \rho K_\alpha^\dagger(t)]. \tag{5}$$

The auxiliary operator K_α responsible for dissipation is formally given by

$$K_\alpha(t) = \int_0^t d\tau C_\alpha(t-\tau)G(t,\tau)Q_\alpha G^\dagger(t,\tau), \tag{6}$$

where

$$G(t,\tau) = \exp_+\left[-i\int_\tau^t dt' H(t')\right], \tag{7}$$

is the Hilbert-space Green's function for the deterministic Hamiltonian of Eq. (3a). Equation (5) results from the second-order cumulant expansion in the system–bath interaction.[34] In the absence of an external field, the second-order cumulant formalism is exact for the spin–boson or boson–boson Hamiltonian in which a two-level or harmonic system interacts linearly with a harmonic bath.[38] Equations (5)–(7) confirm that the dissipation tensor $\mathcal{R}$ in Eq. (1) does depend on the driving field.

Equation (5) involves no computationally tedious tensor manipulation. This is one of the major advantages of Eq. (5) in comparison with the ordinary GME [Eq. (1)]. Further, it constitutes the foundation of the GQFP formulation[34] which will be presented in Sec. IV. Moreover, Eq. (5) provides a way to the classification of dissipation in terms of the dissipative mode Q_α without invoking any specific representation.

B. Classification of dissipation modes

There are two types of dissipation involving energy (T_1-type) and phase relaxation (T_2-type), respectively. The introduction of these types of dissipation is traditionally based on a specific state representation of the reduced density operator ρ. Here the diagonal elements ρ_{aa} are the state populations, while the off-diagonal elements ρ_{ab} are the coherences. In this case, the T_1- and T_2-types may also be referred to as the relaxation of populations and coherences, respectively. As ρ is positive definite and satisfies the Schwarz inequality,[39] $|\rho_{ab}|^2 \leqslant \rho_{aa}\rho_{bb}$, population relaxation induces also the destruction of coherence. On the other hand, one can have a *pure* T_2-type dephasing which involves only the destruction of coherence ρ_{ab} but has no effect on the populations ρ_{aa} and ρ_{bb}. Note that the above concept of T_1- or T_2-type dissipation is introduced through a specific representation and, therefore, is basis set dependent. If one is interested in energy dissipation one should use the energy representation of the density operator.[17]

Next we outline a way for classification of the types of dissipation via the nature of the dissipative mode Q_α without using any representation. For simplicity, we shall consider only the reduced system in the absence of external field. Note that due to the translational invariance, as it should be for Eq. (1), two dissipative modes, Q_α and Q'_α, that differ by a nontrivial *c*-number are considered to be identical.

Let us consider pure T_2-type dephasing and denote the associated dissipative mode as Q_2. Physically, a pure dephasing process refers to dissipation which involves no energy loss. This condition can be expressed as $d\langle E\rangle/dt = \mathrm{Tr}[H_0\dot{\rho}^{(0)}(t)]=0$. Here, H_0 and $\rho^{(0)}$ are the Hamiltonian and reduced density operator, respectively, in the absence of external field. By using Eqs. (5) and (6) with the field-free Hamiltonian H_0, we obtain the following necessary and sufficient condition for a pure dephasing mode:

$$[H_0, Q_2] = 0. \tag{8}$$

Equation (8) is equivalent to say that a pure dephasing mode Q_2 and the field-free Hamiltonian H_0 can be diagonalized simultaneously. The simplest pure dephasing mode that will be used later for numerical application is $Q_2=H_0$. Dissipation modes that do not commute with H_0 will involve energy redistribution. In the energy representation the diagonal elements of Q_α are responsible for the pure dephasing, while the off-diagonal elements give the energy relaxation rates (cf. Sec. IV below).

III. A GENERALIZED QUANTUM FOKKER–PLANCK THEORY WITH MARKOVIAN DISSIPATION

The Langevin GME [Eq. (5) with Eq. (6)] is an integro-differential equation whose numerical solution is in general tedious and time consuming. As mentioned in Sec. I, there are two major theoretical approaches to the further development of a numerically tractable formulation of quantum dissipation. One is the Redfield approach[17,22–24] in which Eqs. (5) and (6) are used directly to establish the relationship among various dissipation tensor elements. Another is the GQFP approach[28–34] which establishes coupled equations of motion for ρ and the hierarchical set of operators, $\{K_{\alpha m}; m=0,\ldots,M\}$ for each dissipative mode Q_α [$K_{\alpha 0}\equiv K_\alpha$ in Eq. (6)].

In the following we shall focus on the correlated influence of driving and Markovian dissipation in molecular systems. In the Markovian limit, an expression for the leading

auxiliary operator K_α [Eq. (6)] may be obtained at least approximately [e.g., Eq. (9) with Eq. (11)]. Let us introduce a rescaled K_α as follows:

$$\tilde{Q}_\alpha(t) \equiv K_\alpha(t)/\eta_\alpha . \tag{9}$$

Here, η_α is the Markovian parameter for the system–bath coupling strength in the given dissipative mode Q_α. Note that the parameter η_α used in this paper corresponds to $\eta_\alpha k_B T$ in Ref. 28 and in our previous work.[34] We can thus recast Eq. (5) into the form

$$\dot{\rho} = -i[H(t),\rho] - \sum_\alpha \eta_\alpha [Q_\alpha, \tilde{Q}_\alpha(t)\rho - \rho \tilde{Q}_\alpha^\dagger(t)]. \tag{10}$$

Given an expression for $\tilde{Q}_\alpha(t)$, the above single GQFP equation can then be analyzed in terms of Redfield dissipation tensor elements in the energy representation (cf. Sec. IV).

Next we propose the following ansatz for the Markovian $\tilde{Q}_\alpha(t)$ [Eq. (9) with Eq. (6)]

$$\tilde{Q}_\alpha(t) = e^{-\beta \mathcal{L}(t)/2} Q_\alpha \equiv e^{-\beta H(t)/2} Q_\alpha e^{\beta H(t)/2}. \tag{11}$$

Here, $\mathcal{L}(t)\bullet \equiv [H(t),\bullet]$ is the Liouville superoperator. Obviously, $\tilde{Q}_\alpha$ is non-Hermitian. Its time dependence arises from the external field which also effects the Markovian dissipation dynamics.[8] For the sake of clarity we shall in the following formal discussion assume that H is time independent.

Equation (11) can be rationalized as follows: Firstly, Eq. (11) reproduces the exact detailed balance condition as the stationary density operator corresponds to the Boltzmann distribution, $\rho_{\rm eq} \propto e^{-\beta H}$. This is easily shown using [cf. Eq. (11)] $\tilde{Q}_\alpha \rho_{\rm eq} - \rho_{\rm eq} \tilde{Q}_\alpha^\dagger = 0$. Secondly, in the Caldeira–Leggett Fokker–Planck equation[28] $\tilde{Q}$ assumes the form [cf. Eq. (5.12) in Ref. 34]

$$\tilde{Q}_\alpha^{\rm CL} \equiv \{1 - \beta \mathcal{L}/2\} Q_\alpha . \tag{12}$$

Both, $\tilde{Q}_\alpha^{\rm CL}$ [Eq. (12)] and $\tilde{Q}_\alpha$ [Eq. (11)], may be considered as resulting from certain first-order expansions with respect to the parameter $\beta H(t)/2$ or $\beta \mathcal{L}(t)/2$. While the former derives from a Taylor series the latter stems from a cumulant expansion. As a first-order Taylor expansion, the Caldeira–Leggett Fokker–Planck equation fails when $k_B T$ is smaller than the energetic bandwidth of the system.[28] In the other hand, $\tilde{Q}_\alpha$ [Eq. (11)] is in the first-order cumulant form which fulfills detailed balance at arbitrary temperature. In this sense, Eq. (10) with Eq. (11) may be viewed as a modification of the Caldeira–Leggett Fokker–Planck equation ensuring detailed balance. It is also worth to mention here that the ansatz Eq. (11) may be derived via an appropriate Markovian limit of the Gaussian–Markovian Fokker–Planck formulation.[40]

Thirdly, the widely used Redfield theory of quantum dissipation can also be written in the form of Eq. (10) with the following auxiliary operator:[24]

$$\tilde{Q}_\alpha^{\rm R} = \frac{2}{e^{\beta \mathcal{L}} + 1} Q_\alpha . \tag{13}$$

The prefactor guarantees that Redfield theory satisfies detailed balance. In fact there is a class of detailed balance preserving auxiliary operators; $\tilde{Q}_\alpha$ [Eq. (11)] and $\tilde{Q}_\alpha^{\rm R}$ [Eq. (13)] are just two examples.[35]

Finally, we note that for a pure dephasing mode Q_2 [cf. Eq. (8)], one has $\tilde{Q}_2 = \tilde{Q}_2^{\rm CL} = \tilde{Q}_2^{\rm R} = Q_2$. The physical reason for this equivalence is that pure dephasing introduces no energy change and, therefore, does not lead to equilibration. In passing we note that this equivalence can be considered as the criterion for any dissipation formulation to be capable to distinguish between the T_1- and the T_2-type of dissipation.

Equations (10) and (11) constitute the final Markovian GQFP formulation of this paper. This result will be used in Sec. V for the numerical study of intramolecular hydrogen transfer in a model system. We have also presented the generalized Redfield theory,[8] i.e., Eqs. (10) where $\tilde{Q}_\alpha$ is replaced by $\tilde{Q}_\alpha^{\rm R}$ [Eq. (13)]. The theoretical development of the detailed balance preserving auxiliary operator class to which $\tilde{Q}_\alpha$ and $\tilde{Q}_\alpha^{\rm R}$ belong will be presented elsewhere.[35] The modified Markovian GQFP [Eqs. (10) and (11)] and the generalized Redfield theory [Eq. (10) with Eq. (13)] are numerically essentially the same for the systems studied in Sec. V. However, the GQFP's $\tilde{Q}_\alpha$ can be considered as the propagation of Q_α in the imaginary time domain ($t = -i\beta$). The resulting GQFP formulation Eq. (10) may thus be implemented not just in the energy eigenstate representations, but also by using numerical grids in coordinate and momentum space.

IV. MARKOVIAN GQFP EQUATION IN THE ENERGY REPRESENTATION

In this section, we shall write the Markovian GQFP equation, Eq. (10), in the energy representation $\{|a\rangle\}$, and then carry out the analysis of the secular Redfield dissipation tensor elements.[23] To simplify the notation, we shall hereafter omit the index α and consider only a single dissipative mode Q explicitly. In the presence of a time-dependent field, the basis set $\{|a\rangle\}$ consists of the *instantaneous* eigenstates of $H(t)$. In this case, the transition frequencies ω_{ab} and Redfield tensor elements $R_{ab,cd}$ become time dependent.

Equation (10) in the energy eigenstate representation $\{|a\rangle\}$ can be recast in terms of Redfield relaxation tensor elements as follows:[23]

$$\dot{\rho}_{ab}(t) = -i\omega_{ab}\rho_{ab}(t) - \sum_{cd} R_{ab,cd}\rho_{cd}(t). \tag{14}$$

Here

$$R_{ab,cd} = \eta \delta_{db} \sum_e Q_{ae}\tilde{Q}_{ec} + \eta \delta_{ac} \sum_e Q_{eb}\tilde{Q}_{ed}^* - \eta Q_{db}\tilde{Q}_{ac} - \eta Q_{ac}\tilde{Q}_{bd}^*, \tag{15}$$

with [cf. Eq. (11)]

$$\tilde{Q}_{ab} = e^{-\beta\omega_{ab}/2} Q_{ab} . \tag{16}$$

Each individual element of the Redfield relaxation tensor $R_{ab,cd}$ in Eq. (15) has a clear physical meaning.[17,23,24] We shall in the following focus on $R_{aa,bb}$ responsible for level

relaxation, and $R_{ab,ab}$ leading to dephasing. The off-diagonal elements Q_{ab}; $a \neq b$, of the dissipative mode yield the T_1-type relaxation, while the diagonal elements Q_{aa} cause pure dephasing (cf. Sec. II B).

Let us first consider $R_{aa,bb}$ and the related properties of population relaxation. Using Eq. (15), we obtain

$$R_{aa,bb} = -2\eta |Q_{ab}|^2 e^{-\beta\omega_{ab}/2}, \quad \text{for } a \neq b. \tag{17}$$

Physically, $-R_{aa,bb}$ is the rate for the $|a\rangle \leftarrow |b\rangle$ transition. It is a T_1-type relaxation rate and is proportional to $|Q_{ab}|^2$. (cf. Sec. II B). Equation (17) leads directly to the detailed balance condition

$$\frac{R_{aa,bb}}{R_{bb,aa}} = e^{-\beta\omega_{ab}}. \tag{18}$$

As $-R_{bb,aa}$ is the rate for the $|b\rangle \leftarrow |a\rangle$ transition, the total relaxation rate associating to the $|a\rangle$ state is then given by

$$\gamma_a = -\sum_b{}' \, R_{bb,aa}. \tag{19}$$

Here, the prime indicates that the summation runs over all $b \neq a$. We can also show that $\gamma_a = R_{aa,aa}$, or $\Sigma_b R_{bb,aa} = 0$ (matter conservation law[41]). Equations (17)–(19) constitute the complete set of relaxation rates in the conventional master equation that involves only population transfer.

We shall now turn to the dephasing tensor element $R_{ab,ab}$. By using Eqs. (15), (17), (19), together with some elementary algebra, we obtain

$$\begin{aligned} R_{ab,ab} &= R^{(1)}_{ab,ab} + R^{(2)}_{ab,ab} \\ &= (\gamma_a + \gamma_b)/2 + \eta (Q_{aa} - Q_{bb})^2. \end{aligned} \tag{20}$$

This recovers the celebrated relation[41] in which the total dephasing rate is a sum of two contributions, the T_1-induced dephasing rate $R^{(1)}_{ab,ab}$ [the first term in Eq. (20)], and the pure dephasing contribution $R^{(2)}_{ab,ab}$ [the second term in Eq. (20)].

In the following section we shall numerically investigate the effect of quantum dissipation on a model intramolecular hydrogen transfer system in the presence of external driving field. Two types of dissipative modes Q will be considered. First the system–bath coupling is taken to be linear in the system coordinate, $Q = x$. In this case both terms in Eq. (20) will give contributions since the considered model system is not harmonic. The second type of dissipation is a pure dephasing in which we choose $Q = H_0$. In this case, only the second term in $R^{(2)}_{ab,ab}$ [Eq. (20)] is nonzero. For this pure dephasing mode, we have actually $R^{(2)}_{ab,ab} = \eta\omega^2_{ab}$.

V. NUMERICAL RESULTS

A. The model

In Ref. 42 some general requirements on an intramolecular hydrogen transfer system favorable for laser control have been discussed. An important point in this respect was that reactant and product configurations should be nonequivalent. One class of molecules which meets this restriction are β-thioxoketones. For a particular case, i.e., thioacetylacetone, we have recently reported high level ab initio calculations which culminated in a two-dimensional potential energy surface.[43] One coordinate describes the hydrogen transfer itself, and the second one simulates the influence of those heavy atom scaffold vibrations which modulate the hydrogen transfer distance most effectively. For the remaining degrees of freedom a harmonic bath model characterized by a continuous spectral density was introduced. In Ref. 9, the hydrogen transfer coordinate was treated explicitly, while the effective heavy atom mode was incorporated in a non-Markovian bath and treated nonperturbatively via the real-time path integral approach.[2]

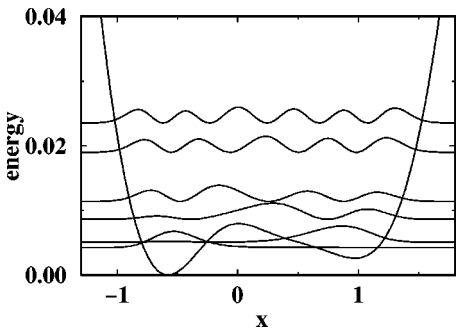

FIG. 1. One-dimensional potential curve, $V(x)$ for isomerization in thioacetylacetone. The parameters entering Eq. (21) are: $k_1 = 5.95$ mD/Å, $k_2 = 4.31$ mD/Å, $x_{0,1} = -0.38$ Å, $x_{0,2} = 0.64$ Å, $\Delta_1 = 0$, $\Delta_2 = 0.0975$ eV, $k_c = 4.24$ eV, and $x_c = 0.152$ Å. The barrier height is 0.214 eV and the asymmetry is 0.07 eV. For details see Ref. 43. The six lowest vibrational eigenfunctions are shown with a vertical offset corresponding to the respective eigenenergies (energies and reaction coordinate are given in atomic units).

In the following we shall apply Eqs. (10) and (11) to the laser driven hydrogen atom switching in thioacetyelacetone within a single reaction coordinate model. The empirical one dimensional potential function for this system is suggested as[9,43]

$$V(x) = V_+(x) - \sqrt{V_-^2(x) + K^2(x)}, \tag{21a}$$

with

$$V_\pm(x) = \tfrac{1}{2}[V^{(1)}_{\rm osc}(x) \pm V^{(2)}_{\rm osc}(x)]. \tag{21b}$$

This form reproduces the energetics at the stationary points as well as the different local vibrations on the reactant (O–H) and product (S–H) side. In Eq. (21), $V^{(i)}_{\rm osc}(x) = k_i(x - x_{0,i})^2/2 + \Delta_i$, are local diabatic potentials which are coupled via the function $K(x) = 2k_c e^{-(x-x_c)^2}$.

Figure 1 depicts the adiabatic potential $V(x)$. The parameters of potential are listed in the figure caption. We also plotted the first six vibrational eigenstates which will be included in the numerical propagation. In the following, the laser driven hydrogen transfer dynamics in the presence of dissipation will be studied at the room temperature. The thermal equilibrium occupations are evaluated to be $\{\rho_{00}, \rho_{11}, \rho_{22}, \ldots\}_{\rm eq} = \{0.705, 0.287, 0.07, \ldots\}$. The dipole moment $\mu = \mu(x)$ is fitted to a linear function interpolating between the values 4.27 and 3.75 Debye obtained for the two stationary points (not shown).[43]

Note that the two lowest eigenstates are rather localized and energetically far below the reaction barrier. This implies that upon changing the occupation probability of these two

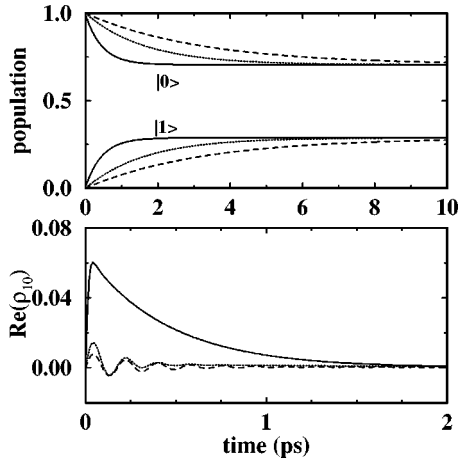

FIG. 2. Population and coherence dynamics of the two lowest eigenstates $|0\rangle$ and $|1\rangle$. The initial state is chosen as the pure state $\rho(t=0)=|0\rangle\langle 0|$. (solid: $\eta_r=1.17$; dotted: $\eta_r=0.12$; dashed: $\eta_r=0.06$). Note that $\rho_{00}+\rho_{11}\approx 1$.

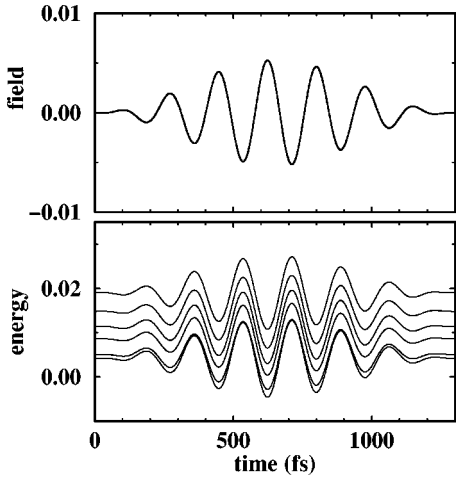

FIG. 3. The IR driving field (upper panel, in atomic units) is shown together with the six lowest instantaneous eigenvalues (lower panel, in atomic units); for parameters see text.

states away from the equilibrium, one effectively modifies the probability distribution for the hydrogen atom's wave function. The external strong laser fields used in Sec. V C will drive the system from the initial $|0\rangle$ state to the final target $|1\rangle$ state. A photoinduced isomerization is thus established. For clarity, the initial reduced density matrices in the following calculations are all chosen as $\rho(0)=|0\rangle\langle 0|$.

B. Field-free dynamics

In the Markovian limit, the strength of system–bath interaction is measured by the friction parameter η. In order to calibrate η with the time scale it implies, we investigate the dissipation dynamics in the absence of the external field. Let us first consider the dissipative mode $Q=x$. With the eigenstates (cf. Fig. 1), we evaluate the dephasing rate γ_a by using Eqs. (17) and (19). We obtain $\gamma_0=0.045\eta$ and $\gamma_1=0.126\eta$. The relaxation-induced dephasing rate, i.e., the first term in Eq. (20), is $R^{(1)}_{10,10}=(\gamma_1+\gamma_0)/2=0.086\eta$. The pure dephasing contribution, i.e., the second term in Eq. (20), is found to be $R^{(2)}_{10,10}=1.55\eta$ that is much larger than $R^{(1)}_{10,10}$. Note that if the potential were symmetric, Q_{aa} and Q_{bb} and thus $R^{(2)}_{ab,ab}$ would be zero in the case of $Q=x$. A large $R^{(2)}_{10,10}$ is apparently due to the asymmetry of the present potential. The dynamics for three different values of η is presented in Fig. 2(a). Here and in the following we will give the coupling strength in units of the transition frequency ω_{10}, i.e., we define $\eta_r=\eta/\omega_{10}$ ($\hbar\omega_{10}=0.853$ mhartree). Apparently, the time scale for relaxation ranges from about 2 ps for $\eta_r=1.17$ to more than 10 ps for $\eta_r=0.06$.

In the absence of dissipation there would be no dynamics since the present initial state is an eigenstate of the field-free Hamiltonian. The coupling to the environment introduces two effects, population relaxation and mixing between populations and coherences by the nonsecular terms in the relaxation matrix. This effect can be seen in Fig. 2(b) where we plotted $\mathrm{Re}\,\rho_{10}(t)$. The behavior changes from an oscillatory one at small η_r to an exponentially decaying one at large η_r, indicating the strong suppression of coherence with increasing friction strength. We note, however, that the initial amplitude of $|\rho_{10}|$ increases with increasing coupling strength. This can be understood in terms of the Schwarz inequality which for short times is approximately, $|\rho_{10}|^2\approx\rho_{00}\rho_{11}$. Thus the stronger the system–bath coupling the larger the population transfer at short times, i.e., the larger the product $\rho_{00}\rho_{11}$.

C. Laser–driven dissipative dynamics

It has been shown that different laser pulse forms can actually switch the populations of the two lowest eigenstates in the present model system.[9] Here we shall use two pulse forms. One is an IR (infrared) pulse tuned into resonance, $\Omega=\omega_{10}$, with the $1\leftarrow 0$ transition

$$\mathcal{E}_1(t)=\mathcal{E}_0\sin^2(\pi t/\tau)\cos(\Omega t),\quad \text{for } 0<t<\tau. \tag{22}$$

For the pulse length of $\tau=1300$ fs and an amplitude of $\mathcal{E}_0=5.2$ mhartree/a_0, an almost perfect transition is achieved in the dissipation free case.[9] Another pulse is the so-called half-cycled (HC) pulse

$$\mathcal{E}_2(t)=\mathcal{E}_0\sin(t\pi/\tau),\quad \text{for } 0<t<\tau. \tag{23}$$

For $\mathcal{E}_0=-6.4$ mhartree/a_0 and $\tau=570$ fs, this field causes also a perfect population switching. (Note that $\mathcal{E}_0$ is negative in order to compensate for the negative sign of the dipole gradient.) However, the mechanism of the control switching with the HC pulse is rather different from that with the IR pulse. While the IR pulse induces a transition between the zeroth-order states, the HC pulse can be viewed as a limit of a so-called tunneling pulse.[43] The latter first creates a localized superposition of zeroth-order eigenstates in a switch-on period. In the following plateau phase the dynamics proceeds as tunneling. Finally, switching-off the field at the right moment stabilizes the wave packet in the product well, i.e., in the present case as the $|1\rangle$ state. The duration of the plateau period for the half-cycled pulse is essentially zero.

Turning to the IR pulse [Eq. (22); shown in Fig. 3(a)] we first calculate the instantaneous eigenvalues [Fig. 3(b)] of the time-dependent Hamiltonian. The most dramatic ac-Stark ef-

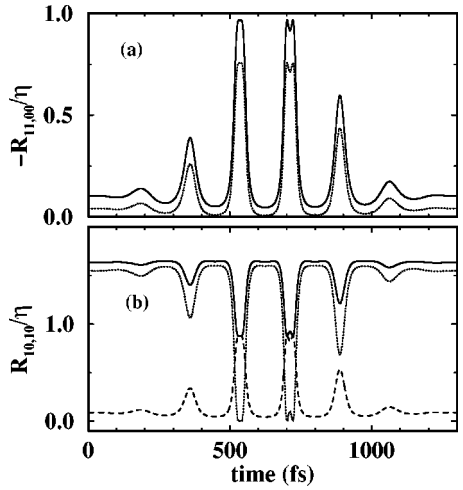

FIG. 4. Field-dressed Redfield dissipation tensor elements. Panel (a) shows $R_{00,11}$ (solid) and $R_{11,00}$ (dotted), respectively, while in panel (b) $R_{10,10}$ is plotted. Presented in (b) are also the T_1-induced dephasing rate (dashed) and the pure T_2 contribution (dotted) to the full dephasing rate (solid).

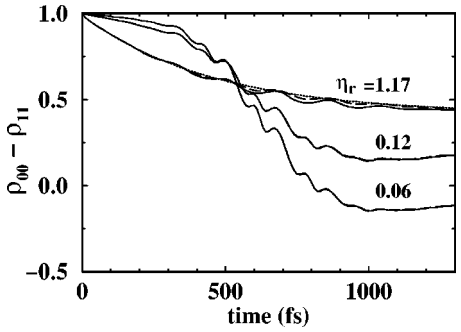

FIG. 5. Population dynamics in field-free energy states for the IR driving at different values of the system–bath coupling strength. The results for the exact time-dependent relaxation rates (solid) are compared with the ones for time-independent rates (long dashes). The bare relaxation dynamics for $\eta_r = 1.17$ without driving is shown as a dotted line.

fect is experienced by the two lowest field-dressed eigenenergies which are getting very close to each other. The respective instantaneous wave functions will be delocalized in this case giving rise to effective transfer of occupation probability between the zeroth-order states.

In Fig. 4(a) we plot the instantaneous relaxation rates $R_{00,11}(t)$ (solid curves) and $R_{11,00}(t)$ (dotted curves) for $Q=x$. First we notice that the rates fulfill detailed balance at every instant of time. Further, the time dependence of the energy gap between the instantaneous states is reflected in the oscillation of these rates which attain their largest values around the maximum of the pulse envelope. The dip seen in the time dependence of the rates around 700 fs (close to the pulse maximum) is due to the fact that the two lowest instantaneous eigenstates approach each other twice [see Fig. 3(b)].

The instantaneous dephasing rate $R_{10,10}(t)$ is plotted in Fig. 4(b) for $Q=x$ together with its T_1-induced and pure T_2 components as calculated, respectively, from the two terms in Eq. (20). It is noteworthy that the pure dephasing component becomes very small in the vicinity of the pulse maximum where the driving field basically compensates for the asymmetry of the potential. This gives $x_{aa} \approx x_{bb} \approx 0$ and the instantaneous pure dephasing rate vanishes approximately according to the second-term of Eq. (20).

The transfer dynamics in the field-free energy representation are shown in Fig. 5 for different values of η_r (note that $\rho_{00}+\rho_{11} \approx 1$). For $\eta_r=0$ the pulse is capable of inducing a complete population switching between the two lowest zeroth-order states (not shown). Increasing the system–bath coupling strength η_r deteriorates this result. The dashed curves in Fig. 5 are evaluated by using the field-free dissipation rate formalism, i.e., setting $H(t) \equiv H_0$ in Eq. (11). Except for the strongest coupling, $\eta_r = 1.17$, used in this study, the population dynamics evaluated via the time-dependent and the time-independent rates are essentially identical. In view of this rather small effect one may expect that the time scale for the change of the energy spectrum by the laser field is much shorter than the respective relaxation time. In other words, if the field would change more slowly, the time dependence of the rates should give a larger effect.

To investigate this point further we consider the case of the HC pulse [Eq. (23)]. In Fig. 6 the pulse is shown together with the instantaneous eigenstates. As in the case of the IR pulse (cf. Fig. 3), only the two lowest states approach each other. This gives rise to a time dependence of the rates similar to the one observed in Fig. 4 in the vicinity of the laser pulse maximum (not shown).

In Fig. 7 the respective population transfer dynamics of the field-free states are shown for different values of η_r. The dissipative mode is chosen as $Q=x$. We first notice that for the same η_r the overall reaction yield with the HC-field is higher than its IR counterpart (cf. Fig. 5). It may be due to the fact that the HC-pulse is much shorter than the IR-pulse, and therefore the dissipation has a smaller influence. Further, the expected difference between the dynamics incorporating time-dependent and time-independent rates is observed already for weak couplings. The relaxation towards the instantaneous eigenstates is more pronounced for stronger coupling. In terms of population transfer in the field-free eigenstates, the relative ordering between the exact and the approximate results exhibits a crossover at about $\eta_r = 0.35$.

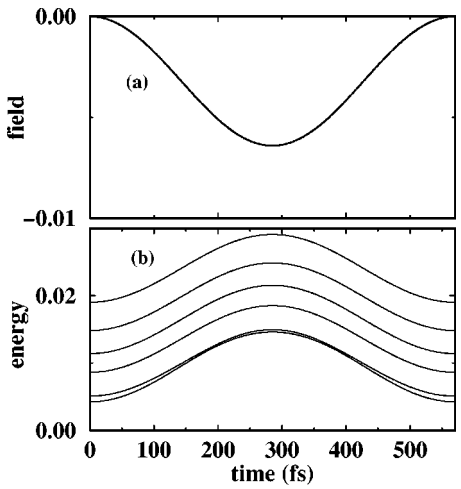

FIG. 6. HC driving pulse (a) together with the instantaneous eigenenergies (b) (in atomic units; for pulse parameters see text).

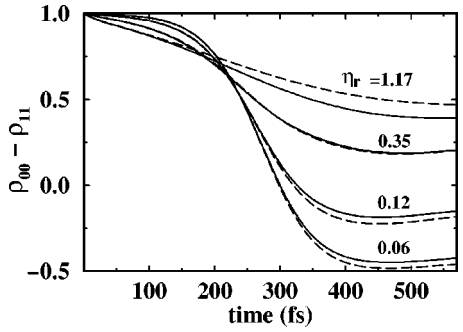

FIG. 7. Population dynamics of the zeroth-order states for HC-pulse driving and different values of the system–bath coupling strength. The results for the exact time-dependent relaxation rates (solid) are compared with the ones for time-independent rates (long dashes).

Finally, we investigate the effect of pure dephasing, i.e., $Q=H_0$, on the IR laser driven dynamics. The pure relaxation rates, $R^{(2)}_{01,01}$ have a similar behavior as the pure relaxation contribution in the case $Q=x$ shown in Fig. 4. In order to facilitate comparison we have chosen different η_r for the two cases, adjusting the value such that the rates $R^{(2)}_{01,01}$ are identical. The population dynamics of the zeroth-order states is shown in Fig. 8 where we also plot the $Q=x$ case for comparison. For small η_r the dynamics with $Q=H_0$ and $Q=x$ is comparable except that after the pulse is switched-off the populations in the $Q=H_0$ case stay constant. For high η_r, however, there is a remarkable difference between the two cases. The yield in the case $Q=x$ is much higher than for $Q=H_0$. This is due to the fact that energy relaxation towards the instantaneous states dominates the dynamics for $Q=x$. This acts in part into the desired direction while for $Q=H_0$ only the phase coherence necessary for establishing the switching between the zeroth-order states is destroyed.

VI. SUMMARY

We have investigated the concerted action of dissipation and laser driving on a reaction coordinate interacting with a thermal bath. The generalized quantum Fokker–Planck equation approach was used in the Markovian limit. The numerical application was performed for a model isomerization reaction by using a one-dimensional description of the intramolecular hydrogen atom transfer in thioacethylacetone. The inclusion of relaxation according to the instantaneous vibrational spectrum was shown to be important for a correct estimate of the reaction yield. This effect depends on the relation between relaxation and laser pulse time scales as illustrated in Sec. IV. We further investigated the separate influence of energy relaxation and pure dephasing type of dissipation. Here we found that energy relaxation taking place on a time scale comparable to the time scale of the laser pulse might act in favor of reaction control. This is not the case for pure dephasing.

In summary, the proposed generalized quantum Fokker–Planck equation method is capable of modeling laser driven dissipative dynamics of multilevel systems. The approximations which are involved in the present treatment, have to be judged against the restrictions imposed by more accurate methods such as the path integral approach. It goes without saying, however, that the applicability of the method has to be confirmed for the system at hand. But, the relatively easy implementation of the proposed method makes it possible, for instance, to include more degrees of freedom into the relevant system. In the case of the hydrogen transfer considered here, this would involve the explicit incorporation of an effective heavy atom mode which modulates the transfer distance.

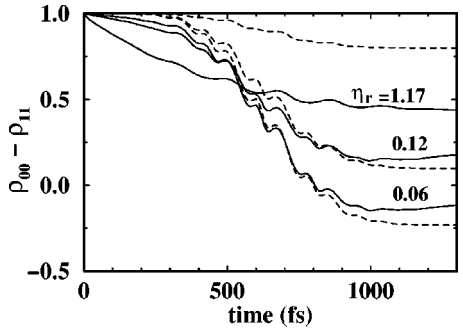

FIG. 8. Population dynamics of the zeroth-order states for IR-pulse driving and different values of the system–bath coupling strength. The results are shown for different models of the system–bath coupling: $Q=x$ (solid) and $Q=H_0$ (dashed). In order to compare the results we have chosen η_r for the $Q=H_0$ model such that the rates $R^{(2)}_{10,10}$ are identical for both models.

ACKNOWLEDGMENTS

This work was financially supported by the Deutsche Forschungsgemeinschaft through the Sfb 450, the DAAD, and by the Research Grants Council of the Hong Kong Government and the National Natural Science Foundation of China. Finally, we would like to thank Professor J. Manz (FU Berlin) for useful discussions and critical comments.

[1] M. Grifoni and P. Hänggi, Phys. Rep. **304**, 29 (1998).
[2] N. Makri, J. Phys. Chem. A **102**, 4414 (1998).
[3] N. Makri, J. Chem. Phys. **106**, 2286 (1997).
[4] N. Makri and L. Wei, Phys. Rev. E **55**, 2475 (1997).
[5] G. Taft and N. Makri, J. Phys. B **31**, 209 (1998).
[6] D. E. Makarov and N. Makri, Phys. Rev. B **52**, R2257 (1995).
[7] L. Gammaitoni, P. Hänggi, P. Jung, and F. Marchesoni, Rev. Mod. Phys. **70**, 223 (1998).
[8] F. Shaung, C. Yang, H. Y. Zhang, and Y. J. Yan, Phys. Rev. E (submitted).
[9] O. Kühn, Eur. Phys. J. D **6**, 49 (1999).
[10] R. I. Cukier, C. Denk, and M. Morillo, Chem. Phys. **217**, 179 (1997).
[11] O. Kühn, D. Malzahn, and V. May, Int. J. Quantum Chem. **57**, 343 (1996).
[12] M. V. Korolkov, J. Manz, and G. K. Paramonov, J. Chem. Phys. **105**, 10874 (1996).
[13] R. W. Zwanzig, J. Chem. Phys. **33**, 423 (1960).
[14] R. W. Zwanzig, *Statistical Mechanics of Irreversibility: Lectures in Theoretical Physics, Vol. III* (Wiley, New York, 1961).
[15] R. W. Zwanzig, Annu. Rev. Phys. Chem. **16**, 67 (1965).
[16] H. Mori, Prog. Theor. Phys. **33**, 423 (1965).
[17] V. May and O. Kühn, *Charge and Energy Transfer Dynamics in Molecular Systems* (Wiley-VCH, Berlin, 2000).
[18] R. Graham and R. Hübner, Ann. Phys. (N.Y.) **234**, 300 (1994).
[19] S. Kohler, T. Dittrich, and P. Hänggi, Phys. Rev. E **55**, 300 (1997).
[20] T. Dittrich, B. Oelschlägel, and P. Hänggi, Europhys. Lett. **22**, 5 (1993).
[21] D. H. Schirrmeister and V. May, Chem. Phys. Lett. **297**, 383 (1998).
[22] F. Bloch, Phys. Rev. **105**, 1206 (1957).
[23] A. G. Redfield, Adv. Magn. Reson. **1**, 1 (1965).
[24] W. T. Pollard, A. K. Felts, and R. A. Friesner, Adv. Chem. Phys. **93**, 77 (1996).
[25] H. Dekker, Phys. Rev. A **16**, 2126 (1977).

[26] H. Dekker, Physica A **93**, 311 (1979).
[27] H. Dekker, Phys. Rep. **80**, 1 (1981).
[28] A. O. Caldeira and A. J. Leggett, Physica A **121**, 587 (1983).
[29] Y. Tanimura and R. Kubo, J. Phys. Soc. Jpn. **58**, 101 (1989).
[30] Y. Tanimura and P. G. Wolynes, Phys. Rev. A **43**, 4131 (1991).
[31] Y. Tanimura and P. G. Wolynes, J. Chem. Phys. **96**, 8485 (1992).
[32] Y. Tanimura and S. Mukamel, J. Chem. Phys. **101**, 3049 (1994).
[33] Y. Tanimura and Y. Maruyama, J. Chem. Phys. **107**, 1779 (1997).
[34] Y. J. Yan, Phys. Rev. A **58**, 2721 (1998).
[35] F. Shuang and Y. J. Yan, J. Chem. Phys. (to be published).
[36] U. Weiss, *Quantum Dissipative Systems* (World Scientific, Singapore, 1993), Series in Modern Condensed Matter Physics, Vol. 2.
[37] D. Chandler, in *Liquides, Cristallisation et Transition Vitreuse; Les Houches, Session LI*, edited by D. Levesque, J. P. Hansen, and J. Zinn-Justin (Elsevier, New York, 1990), pp. 1–101.
[38] *Quantum Statistics in Optics and Solid State Physics. Statistical Treatment of Open Systems by Generalized Master Equations*, edited by F. Haake (Springer, Berlin, 1973), Springer Tracts in Modern Physics, Vol. 66.
[39] E. Merzbacher, *Quantum Mechanics*, 2nd ed. (Wiley, New York, 1970).
[40] F. Shuang, H. Y. Zhang, and Y. J. Yan (unpublished).
[41] N. G. van Kampen, *Stochastic Processes in Physics and Chemistry* (North-Holland, Amsterdam, 1992).
[42] N. Došlić, O. Kühn, and J. Manz, Ber. Bunsenges. Phys. Chem. **102**, 292 (1998).
[43] N. Došlić, K. Sundermann, L. González, O. Mó, J. Giraud-Girard, and O. Kühn, Phys. Chem. Chem. Phys. **1**, 1249 (1999).